J. Fluid Mech. (1992), *vol.* 245, *pp.* 301–317

Higher-order Bragg reflection of gravity surface waves by periodic beds

By ELISABETH GUAZZELLI,[1] VINCENT REY[2] AND MAX BELZONS[2]

[1] Laboratoire de Physique et Mécanique des Milieux Hétérogènes, URA 857 du CNRS, ESPCI, 10 rue Vauquelin, 75231 Paris Cedex 05, France

[2] Département de Physique des Systèmes Désordonnés, SETT, URA 1168 du CNRS, Université de Provence, Centre de Saint-Jérôme, Case 161, 13397 Marseille Cedex 13, France

(Received 13 June 1991 and in revised form 3 June 1992)

Experiments are described which demonstrate higher-order Bragg resonant interactions between linear gravity waves and doubly sinusoidal beds. These higher-order effects, which include harmonic and subharmonic Bragg reflections, have been observed by making very precise measurements in a wave tank. Subharmonic reflection was found to be very large, even for small bottom undulation amplitudes. The experimental data are compared with the predictions of a numerical model based on the full potential theory of linear waves.

1. Introduction

In recent years, the interaction of surface gravity waves with a periodic bottom has been studied extensively, both experimentally and theoretically. For waves which are normally incident on a region of long-crested sinusoidal undulations, the result of principal interest has been the resonant reflection of the incident waves when the surface wave wavenumber (k) is half the bed wavenumber (K), that is, $K = 2k$. This wave reflection, which is due to the multiple interferences of the waves from the periodic scattering centres, has been well known in solid-state physics as Bragg reflection for about sixty years. It corresponds to the first forbidden band found by Brillouin in the quantum theory of solids: the energy in the forbidden range is totally reflected by a regular lattice (see for example, Kittel 1976).

In the rather different context of oceanography, an important application of the Bragg effect relates to the patches of sand bars which are commonly formed off beaches, outside the breaker zone, with wavelength of the order of 100 m. Such bars are capable of partially reflecting incident waves having the appropriate wavelength, thereby, protecting the beach-face from the full impact of the waves (see for example, Bailard *et al.* 1990; Bailard, DeVries & Kirby 1992). Moreover, on a fully erodible sand bed, a 'coupling' may arise between the reflection of incident wave energy and the growth of new sand bars (see for example, Carter, Liu & Mei 1973; Short 1975; Heathershaw & Davies 1985; Benjamin, Boczar-Karakiewicz & Pritchard 1987; O'Hare & Davies 1990).

The case of linear surface waves incident upon a horizontally one-dimensional sinusoidal bottom of finite extent was examined by Davies (1982*a*) and Davies & Heathershaw (1984). The method of regular perturbation expansions was used to solve the linear potential equations of waves in which the ratio ϵ of the bottom amplitude ΔH to the mean water depth H_0 was taken as a small parameter. The

reflection coefficient R (defined as the quotient of the reflected and incident wave amplitudes) displays a resonant Bragg peak centred around $2k/K = 1$. In addition, the reflection coefficient oscillates in the ratio of total length L of the sinusoidal bed to the surface wavelength. This latter effect was demonstrated for rectangular obstacles by Mei & Black (1969).

At resonance ($2k/K = 1$), as the number M of ripples in the patch becomes larger, the reflection coefficient of Davies & Heathershaw (1984) becomes unbounded, and the perturbation theory breaks down (the case of an infinite sinusoidal bottom was also studied by Davies 1982*b* and Mitra & Greenberg 1984). In order to overcome this difficulty, Mei (1985) developed a theory appropriate for large reflection which allows the reflected wave to be of the same order as the incident wave. By using a multiple-scales approach, Mei found two equations, uniformly valid in space and time which couple the incident and reflected wave envelopes through the amplitude of the bottom undulations (Klein–Gordon equations). Thus, he obtained a uniformly valid expression for the reflection coefficient in the vicinity of the resonance at $2k/K = 1$.

Davies' results for small R and ϵM and Mei's results at (or close to) resonance, are in good agreement with the experimental data of Heathershaw (1982) and Davies & Heathershaw (1984) obtained for $\epsilon \leqslant 0.30$ and spatial period number, $M = 2$, 4 and 10. Further comparisons with these data have been made by Dalrymple & Kirby (1986) and Kirby (1986). For both resonant and non-resonant cases, Dalrymple & Kirby (1986) used a boundary-integral-equation method to compute numerically the reflection coefficient. Kirby (1986) derived a modified mild-slope equation, found the two coupled equations of Mei (1985) at resonance for a sinusoidal bottom and, by numerical computation, obtained the reflection coefficient. Further comparisons with similar laboratory experiments were reported by Hara & Mei (1987) and Benjamin *et al.* (1987).

The present study concerns the higher-order Bragg effects coming from the large amplitude, or large slope, of bottom undulations and was motivated by some preliminary experiments on a sinusoidal bottom with a spatial period number, $M = 22$ (Guazzelli 1986). For $\epsilon = 0.57$, the plot of the reflection coefficient versus the wave frequency showed both the main Bragg resonant peak in the vicinity of $K = 2k$ and a new second smaller resonant peak in the vicinity of $K = k$. In addition, the former Bragg peak was shifted towards lower frequencies compared with the prediction of the lowest-order theories of Davies (1982*a*) and Mei (1985).

Some explanation of these new higher-order effects can be obtained by considering the simplest available formalism of the linear shallow-water theory. The propagation of long surface waves over a sinusoidal bottom of infinite extent was first discussed by Rhines (1970). Following a similar procedure, the case of a bed of finite extent was examined for the general non-resonant case and for exact resonance by Davies, Guazzelli & Belzons (1989). Under the assumption that the relative bed amplitude and bed steepness are small parameters, the shallow-water equation can be transposed into a Mathieu's equation. The forbidden bands, corresponding to strong reflection of the incident waves by the bottom undulations, appear at $2k/K = 1, 2, 3, 4, \ldots$ (see the Mathieu stability diagram in Abramowitz & Stegun 1965, Chap. 20). In an analysis to lowest order in ϵ, which is consistent with the approximations made in deriving the Mathieu equation, only the first-order Bragg resonance is revealed. Since the widths of the forbidden bands are of order $\epsilon, \epsilon^2, \epsilon^3, \ldots$, the respective higher-order Bragg resonances are revealed successively by an analysis to higher orders in ϵ. As ϵ increases, the widths of the forbidden bands grow, and their centres are displaced from the integral values of $2k/K$ above. This gives a qualitative explanation

for the occurrence of the second-order Bragg resonance around $K = k$, and for the shift of the resonant peaks to lower frequencies than those predicted by linear theory when ϵ is increased. The underlying physical explanation for these effects involves the multiple interference process between the incoming waves and the waves which are partially reflected by each ripple. This is revealed in the long-wave model through the instabilities of the solutions of Mathieu's equation. The results of Davies *et al.* (1989) were extended to intermediate-depth dispersive waves by Kirby (1989).

In the case of a bed consisting of the superimposition of two sinusoids having different wavenumbers K_1 and K_2 and same bed relative amplitudes $\Delta H/H_0 = \epsilon = \epsilon_1 = \epsilon_2$, the shallow-water equation can be transformed by the procedure outlined above into an almost-periodic Mathieu equation. In an analysis to the first order in ϵ, only the first Bragg resonances corresponding to each sinusoid, i.e. $k = \frac{1}{2}K_1$ and $\frac{1}{2}K_2$, are revealed. For larger ϵ, the higher-order Bragg resonances are revealed successively. In an analysis to second order, the second-order bands indicate wave reflection for $k = K_1, K_2$, $\frac{1}{2}(K_2+K_1)$ and $\frac{1}{2}(K_2-K_1)$. The resonances associated with $k = \frac{1}{2}(K_2-K_1)$, which occur at low frequency, are called subharmonic Bragg resonances. Those associated with $k = K_1, K_2$ and $\frac{1}{2}(K_2+K_1)$, which occur at large frequency, are called harmonic Bragg resonances. The centres of the bands are again slightly shifted toward lower frequencies than predicted by the values of $2k/K$ above, when ϵ is increased. More generally, such higher-order resonances may be found in every propagation problem governed by an almost-periodic Mathieu equation. An example is the case of an electromagnetic wave propagating through a medium with an almost periodic permittivity (see, for example, Jaggard & Jordan 1984).

For a sinusoidal bed, the lowest-order analytic theories of Davies (1982*a*, *b*) and Mei (1985) as well as the mild-slope equation approach of Kirby (1986) cannot account for the presence of these new higher-order effects as higher-order Bragg resonances nor the shift toward lower frequencies. For the superimposition of two sinusoids, it is possible, as a first-order approximation, to add the separate contributions given by the first-order theories for each sinusoidal component of the bed (Kirby 1986; Kirby & Anton 1990). However, higher-order effects coming from large bed amplitude cannot again be predicted by these lowest-order theories (Kirby & Anton 1990). Along these lines, it should be noted that C. C. Mei (1988, personal communication) has derived a second-order theory for the resonant reflection by a rippled bed containing two wavenumbers (K_1 and K_2). This theory, which represents an extension of Mei's (1985) approach, reveals the second-order bands ($k = K_1, K_2$, $\frac{1}{2}(K_2+K_1)$ and $\frac{1}{2}(K_2-K_1)$ when the calculation is performed in the vicinity of these bands.

It is possible to describe these higher-order phenomena by using a non-perturbative numerical approach. Indeed, the boundary-integral-equation method used by Dalrymple & Kirby (1986) remains valid for large bed amplitude. They noticed that for a sinusoidal bed with $\epsilon = 0.30$, their computed Bragg peak was slightly shifted towards low frequencies, compared with the peak obtained on the basis of lowest-order perturbation theories.

In the present work, we chose to compare experimental data to predictions of a numerical model based on the linear wave potential theory which describes the wave propagation over a doubly sinusoidal bed (see also, Belzons, Rey & Guazzelli 1991). This model was first proposed by Takano (1960) and was then improved by Kirby & Dalrymple (1983). It describes wave propagation over a series of steps and can be applied to any smooth topography by discretization of the bottom into narrow shelves. The problem of the resonant reflections of waves by sinusoidal and doubly

sinusoidal beds was addressed by Mattioli (1990, 1991) by means of the same numerical model. Mattioli (1990, 1991) investigated the role of the evanescent modes, which are created at each step discontinuity, in the resonant reflection phenomenon. For the case of doubly sinusoidal beds, Mattioli (1991) demonstrated the existence of the first-order Bragg resonant reflections as well as the second-order Bragg resonant reflections. Applications of this model to different bottom topographies, such as rectangular obstacles, sloping and sinusoidal or doubly sinusoidal beds, including a complete justification of the convergence of the results are obtained in Rey (1991, 1992). A comparison between the prediction of this model and experimental data for waves propagating over a single bar can be found in Rey, Belzons & Guazzelli (1992).

We should also mention a model developed by Devillard, Dunlop & Souillard (1988) for wave propagation over a series of steps using the renormalized transfer matrix introduced by Miles (1967). A comparison between this model and the numerical model of Takano (1960) and Kirby & Dalrymple (1983) for the case of waves propagating over a single submerged rounded bar can be found in Rey *et al.* (1992). This model has been also used by O'Hare & Davies (1991) for the case of waves propagating over small-amplitude sinusoidal bottoms. Since this model is, in fact, a variational improvement upon the plane wave approximation, the use of this method for the prediction of the wave field over a series of steps is strictly valid only if the non-propagating modes, which are created at each step discontinuity, are negligible when they reach the preceding or following steps. As a result, this method does not predict accurately the higher-order phenomena for a finitely discretized doubly sinusoidal bed.

Since any periodic bed can be represented by its Fourier components, the present problem is also related to the study of resonant reflection between gravity waves and periodic beds consisting of a series of bars. In this case, not only the first Bragg resonance, around $2k/K = 1$, but also the second resonance, around $k/K = 1$, were experimentally demonstrated by Belzons, Guazzelli & Parodi (1988), for a periodic bed consisting of a series of 29 rectangular bars of relative height 0.43. Comparisons of these data with the numerical method of Takano (1960) and Kirby & Dalrymple (1983) as well as with the numerical method of Devillard *et al.* (1988), derived from Miles (1967), were presented by Rey (1991, 1992). Both methods gave similar predictions in good agreement with the experimental data of Belzons *et al.* (1988), particularly in respect to the position and width of the two resonant peaks. The formation of the second resonance peak was numerically confirmed and examined by Mattioli (1990, 1991). Experiments by Kirby & Anton (1990) with a periodic bed consisting of a series of four bars of relative height 0.33 also showed the first and second Bragg resonant reflections. The experimental data were shifted to lower frequencies compared with the prediction of the lowest-order theories.

In this paper, we present an experimental study of linear gravity surface waves propagating over a bed consisting of the superimposition of two sinusoids having different wavenumbers K_1 and $K_2 > K_1$ and the same bed relative amplitude $\epsilon = \Delta H/H_0$. Our objective in this work is to examine the effects arising from the large amplitude, or large slope, of bottom undulations. To this end, a systematic experimental study of the interactions between linear gravity surface waves and doubly sinusoidal beds was undertaken by gradually increasing the bed relative amplitude ϵ. We expect to observe a reflection of the incoming wave when its wavenumber k satisfies the first-order Bragg conditions corresponding to each sinusoid, i.e. $k = \frac{1}{2}K_1$ and $\frac{1}{2}K_2$, but also the second-order Bragg conditions

corresponding to $k = K_1, K_2$, $\frac{1}{2}(K_2+K_1)$ and $\frac{1}{2}(K_2-K_1)$. Additional aspects of this work related to subharmonic resonant reflection may be found in Belzons *et al.* (1991).

The paper is organized as follows. The theoretical model is outlined in §2 and the experimental techniques in §3. In §4, the experimental results are presented and compared with the numerical calculations, as well as with the predictions of the first-order theory by using the additivity of the separate contributions for each sinusoidal component of the bed. Finally, in §5, the results are discussed and brief conclusions are drawn.

2. Theoretical model

The model is briefly presented in this section and further details can be found in the original papers of Takano (1960) and Kirby & Dalrymple (1983) as well as in Mattioli (1990, 1991), Belzons *et al.* (1991), Rey (1991, 1992) and Rey *et al.* (1992).

2.1. *Mathematical model and numerical method*

The formulation is based on the full potential theory of linear monochromatic waves propagating in one horizontal direction. The flow is assumed to be irrotational. The departure of the water surface from its mean level ($y = 0$) is taken as $\eta(x,t)$ (t is time, x the horizontal axis), and the fixed impermeable bed is defined by $y = H(x)$. The (complex) velocity potential is assumed to have time dependence

$$\Phi(x,y,t) = \mathrm{e}^{\mathrm{i}\omega t}\,\phi(x,y),$$

($f = \omega/2\pi$ is the frequency). The motion is governed by Laplace's equation with a linearized free-surface condition and a bed condition expressing the vanishing of the normal component of the fluid velocity.

The smooth bottom is discretized into a series of N narrow shelves, and the problem reformulated as the propagation of waves over a succession of domains of constant depth separated by small steps. In any domain m of constant depth H_m, the complete solution of Laplace's equation and boundary conditions can be written in the form

$$\phi_m(x,y) = A_m^{\pm}\,\mathrm{e}^{\pm \mathrm{i}k_m(x-x_m)}\,\chi_m + \sum_{n=1}^{\infty} B_{m,n}^{\pm}\,\mathrm{e}^{\pm\kappa_{m,n}(x-x_m)}\,\psi_{m,n}, \tag{1}$$

where the $\mathrm{i}k_m$ are solutions of the dispersion relation $k_m \tanh(k_m H_m) = \omega^2 g^{-1}$, $\kappa_{m,n}$ ($n = 1, 2, \ldots, \infty$) are solutions of the dispersion relation

$$\kappa_{m,n} \tan(\kappa_{m,n} H_m) = -\omega^2 g^{-1},\ \chi_m(y) = \cosh(k_m(H_m - y))$$

and $\psi_{m,n}(\kappa_m, y) = \cos(\kappa_{m,n}(H_m - y))$. Two propagating wave modes are described by the terms with coefficients $A_m^{\pm}$, and infinitely many non-propagating modes at $x = x_m$ are described by the terms with coefficients $B_{m,n}^{\pm}$, $n = 1, 2, \ldots, \infty$. The functions χ_m and $\psi_{m,n}$ form a complete orthogonal set for each region m.

The matching conditions ensuring continuity of both fluid velocity and surface elevation between successive steps can be written. Each matching condition can then be multiplied in turn by all members of the complete orthogonal set $\{\chi_m, \psi_{m,n};\ n = 1, 2, \ldots, \infty\}$ and each resulting equation integrated over the appropriate depth. Infinitely many equations must be considered because of the infinite number of evanescent modes. Therefore, at each step, not only do the two propagating solutions become coupled, but the evanescent modes also become coupled with the propagating ones and among themselves. As a result, the situation is not that of the propagation of a simple plane wave but that of the propagation of an infinite number of coupled

channels. It is, then, the entire set of propagative and non-propagative mode which determines, by means of successive small contributions, the total effect on the incident propagating wave.

In order to solve the problem numerically, the non-propagating modes must be truncated at some order $n = P$. For a bottom consisting of N steps, a direct numerical method requires the simultaneous resolution of $2N(P+1)$ equations for the determination of the $2N(P+1)$ unknown complex coefficients $A_m^{\pm}$ and $B_{m,n}^{\pm}$. We used an additional approximation, consisting of a subdivision of the whole bottom into S smaller subsystems or patches to which the numerical method could be more easily applied.

Each patch has an influence on the wave, which depends on its direction of propagation. The above direct method allows the calculation of the response in terms of reflection and transmission for an incident wave of arbitrary amplitude (propagating towards $x > 0$) and for a retrograde wave of arbitrary amplitude (propagating towards $x < 0$) encountering the patch. Owing to the linearity of the model, we can define and characterize in the same way an equivalent patch composed of two successive patches. For a bed subdivided into S patches, we can proceed by successive iterations. For the bottoms used in the experiments (see §§3 and 4), each bed period was taken as a patch and was discretized into 61 steps of equal length. In order to ensure that the resolution involved no numerical problems, we also checked that the energy conservation was satisfied within an accuracy of 10^{-8}. The major benefits of the patch method are a significant reduction of calculation time as well as the ability to solve very large, finely discretized systems. This method is particularly efficient in the present case because it takes advantage of the periodicity of the bed.

2.2. *Limitations of the numerical model*

There are certain physical limitations of the computations performed in this work which arise from approximations of the potential theory of pure linear gravity waves as well as approximations of the numerical method.

The limitations of the former kind may be stated as a set of simple conditions on the various lengthscales in the problem (see, for example, Whitham 1974):

$$Ak, AH_0^{-1}, Ak^{-2}H_0^{-3} \ll 1, \tag{2}$$

where A is the surface wave amplitude, k is the wavenumber and H_0 is the mean water depth. Moreover, we must verify that the effect of surface tension can be neglected. Another physical limitation is that viscous dissipation is ignored in the model.

An additional limitation of the numerical model comes from the truncation of the evanescent modes. It was numerically verified that in the range of frequencies and depth discontinuities experimentally investigated here, the results for the wave field rapidly converge as the number P of evanescent modes is increased. The model was tested using $P = 0$, 1, 2, 3 and 4 evanescent modes to get a quantitative idea of the rate of convergence of the computation. These tests showed that the results for the reflection coefficient presented below were convergent to within 2% using 3 evanescent modes. Additional justification of the convergence of the results including other bed topographies can be found in Rey (1991, 1992).

Finally, the last numerical limitation comes from subdividing the bed into patches. This approximation is justified if the range of the evanescent modes emitted at the nearest discontinuities on both sides of the separating point is small relative to the distance between these two steps. This range can be evaluated numerically for each

patch independently by calculating the relative contribution of the evanescent terms emitted from each of the two nearest steps. Indeed, one would expect the patch subdivision approximation to be most efficient when the one-period patches are bounded at a crest or trough of the bottom. But, in order to deal with a single patch in our computation, the one-period patches are bounded at a maximum slope location since the bed also starts and ends at a maximum slope point. We have verified that this choice remains correct, as shown on figure 7 where the calculations using a patch subdivision either at the troughs or at the maximum slopes give very similar results. For the maximum slope bed subdivision, we also checked numerically that the relative contribution of the evanescent modes, at patch boundaries, was of the order of 5%.

3. Experimental techniques

3.1. *The wave tank and the periodic bottoms*

The experiments were carried out in a glass-walled wave tank, of length = 4.70 m and width = 0.39 m. The bottom of the tank was levelled so that its deviation from a horizontal plane was within 1 mm, and the width of the channel was uniform to within 1 mm. The average water depth H_0 was varied between 2.5 and 4 cm. Water depths were determined to within an estimated 0.2 mm. Beds composed of periodic corrugations were built into a false flat bottom, extending in the up- and down-wave directions with the mean water depth H_0. These beds were such that the depth varied only in the x-direction along the wave tank so that, apart from weak edge effects, the motion of the wave was horizontally one-dimensional. The beds consisted of the superimposition of two sinusoids having different wavenumbers, K_1 and K_2, such that $H(x) = H_0 - \Delta H_1 \sin(K_1 x) - \Delta H_2 \sin(K_2 x)$. Three different bottom types were used in the experiments. The first bottom, S_1, had amplitudes $\Delta H = \Delta H_1 = \Delta H_2 =$ 1 cm and wavenumbers $K_1 = 0.52$ cm^{-1} and $K_2 = 1.05$ cm^{-1} (i.e. wavelengths $\Lambda_1 =$ 12 cm and $\Lambda_2 = 6$ cm). Two lengths of this bed were studied, having $L = 48$ cm and 192 cm. The second bottom, S_2, had amplitudes $\Delta H = \Delta H_1 = \Delta H_2 = 0.5$ cm and wavenumbers $K_1 = 1.05$ cm^{-1} and $K_2 = 1.57$ cm^{-1} (i.e. wavelengths $\Lambda_1 = 6$ cm and $\Lambda_2 = 4$ cm). The length of this bed was $L = 48$ cm. The last bottom S_3 had the same wavenumbers as S_2, $K_1 = 1.05$ cm^{-1} and $K_2 = 1.57$ cm^{-1} but different amplitudes $\Delta H = \Delta H_1 = \Delta H_2 = 1$ cm. The length of this bed was $L = 48$ cm.

For a distance of 1.10 m up-wave of each of these ripple patches, and between their down-wave ends and the beach, the bed was flat and the water depth constant (H_0). Diminishing the mean water depth increases the relative amplitude of the bottom undulations, characterized by $\epsilon = \Delta H/H_0$. In the following experiments with beds S_1 and S_3, the values studied were $\epsilon = \Delta H/H_0 = 0.25$, 0.33, 0.40 (corresponding to the mean depths $H_0 = 4$, 3 and 2.5 cm). In the experiments with bed S_2, the values studied were $\epsilon = \Delta H/H_0 = 0.13$, 0.17, 0.20 (corresponding to the mean depths $H_0 = 4$, 3 and 2.5 cm).

At one end of the wave tank, a piston-type wave generator created a monochromatic sinusoidal wave of amplitude smaller than 1 mm, resulting in an (incident) wave field which is expressed by $\eta_i(x,t) = A_i(x)\cos(kx - \omega t)$. The vertical paddle of the wave generator was driven by a microstepping motor which was monitored by a microcomputer. The paddle mechanical system ensured a perfect sinusoidal motion of the paddle. This paddle was used to generate wave frequencies $f(= \omega/2\pi)$ in the range 0.7 to 6 Hz. The frequency was determined to an accuracy better than 0.0001 Hz.

At the other end of the tank, a 12°-slope rubberized-fibre wave absorbing beach, and a reservoir filled with the same absorbing material, were built to prevent waves from being back-reflected onto the variable bottom. The length of the beach was $L_B = 70$ cm, the volume of the reservoir was $V_R = 100$ l. Measurements of the back-reflection by the beach are discussed in the following section.

3.2. *Wave measurements*

Measurements of the wave elevation $\eta(x,t)$ were made with an absolute accuracy better than 40 μm using an optical detection technique. The optical devices were mounted on a carriage which could slide along the top of the tank on two rails. The motion of the carriage was controlled through the microcomputer by a stepping motor, which ensured reproducibility of the measuring positions. The smallest available displacement corresponding to one step was 0.0456 mm.

For any given wave frequency, the reflection coefficient R (defined as the quotient of the reflected and incident wave amplitudes) was obtained from measurements of the partially standing wave field between the wave generator and the beginning of the variable bottom. Typically, wave measurements were made at 40 positions for each frequency in order to resolve the wave envelope over a complete surface wavelength, and the entire process was repeated for each frequency examined. The wave measurements were made at distances no less than approximately half a surface wavelength from the start of the region of undulating bottom to ensure that all the non-propagating modes had died out. Wave amplitudes were measured throughout the region of undulating bottom and the harmonic content of the surface wave field was also examined.

In order to obtain the reflection coefficient for the beach in isolation, wave measurements were made on a flat bottom having the same depth as the mean depth used for the present experiments. The measurements were made at the same locations in the wave tank as the present experiments to ensure that the reflected waves were damped by the viscosity in the same way. The beach reflection coefficients were of the order of $R_B = 0.1$–0.2 below about 1.8–2.0 Hz. Above 1.8–2.0 Hz, beach reflection was negligible.

In the middle-frequency range, uncertainties in reflection coefficient measurements are less than few percent. In the low-frequency range ($<$ 1.8–2.0 Hz) backscattering by the beach introduces uncertainties into values of the reflection coefficient. The true value R_T of the reflection coefficient is estimated in the experiments to within a range of uncertainty around the measured value R given by $R_T = R \pm R_B$. At large frequencies, since the wave generator efficiency is poor and the wave viscous damping is large, wave amplitudes are very small and difficult to detect. Therefore, relative uncertainty on the reflection coefficient can reach 40% above 4.5 Hz. Above 4.0–4.5 Hz, since the wave generator efficiency is poor, taking measurement is very difficult and in some cases, measurements were not obtained. This is why some high frequencies are not covered by the experimental data in some figures shown in §4.

Except for the bed types used and some slight modifications to the apparatus, the basic apparatus was the same as that used by Belzons *et al.* (1988) and Rey *et al.* (1992) where further details of the equipment and experimental methods may be found.

4. Experimental results

Before the experiments were carried out, it was verified that the measured waves were linear gravity waves (see condition (2)). Typical wave steepnesses (Ak) were in the range 0.01–0.10, the relative amplitude (A/H_0) was at most 0.05 and the values of the Stokes parameter $A/k^2H_0^3$ were in the range 0.03–0.8. It was also confirmed experimentally, by checking the predictions of the dispersion equation, that the effects of the surface tension were negligible in the frequency range of interest. The investigation of the harmonic content of the surface wave field revealed that more than 98% of the wave elevation was at the fundamental frequency. Thus, the waves examined in the experiments were linear monochromatic gravity waves in either shallow water or water of intermediate depth. Taken together, these considerations justify the use of a numerical model based on the linear potential theory as a basis for comparison with the experimental data.

4.1. *Reflection coefficients for the bed S_1 with $K_1 = \frac{1}{2}K_2$*

Consider the results for the bed S_1 with a length $L = 48$ cm, which corresponds to a spatial period number $M = 4$ for the largest wavelength Λ_1. The plots of R versus f presented in figures 1 and 2 show the effect of an increase in the relative amplitude of the bottom modulation $\epsilon = \Delta H/H_0$. Only data corresponding to $\epsilon = 0.25$ ($H_0 = 4$ cm) and $\epsilon = 0.40$ ($H_0 = 2.5$ cm) are shown. Experiments were also performed for an intermediate value $\epsilon = 0.33$ ($H_0 = 3$ cm) and showed a continuous behavioural change between these two extreme values.

In the figures, the arrows indicate the location of the frequencies f_1, f_2, corresponding respectively to the wavenumbers $\frac{1}{2}K_1$ and $\frac{1}{2}K_2$ (i.e. to the first-order Bragg resonance), as well as the location of the frequencies f_{1+}, f_{2+}, f_- and f_+ which correspond respectively to the wavenumbers K_1, K_2, $\frac{1}{2}(K_2-K_1)$ and $\frac{1}{2}(K_2+K_1)$ (i.e. to second-order Bragg resonances). These frequencies were computed using the dispersion relation over a flat bed for the water depth of interest, H_0. They will be hereafter referred as the plane wave frequencies of the Bragg resonances. It should be noted that, since $K_1 = \frac{1}{2}K_2$ for bed S_1, the second-order bands corresponding to $k = K_1$ and $k = \frac{1}{2}(K_2-K_1)$ cannot be distinguished from the first-order bands $k = \frac{1}{2}K_2$and $k = \frac{1}{2}K_1$, respectively (i.e. $f_- = f_1$ and $f_2 = f_{1+}$).

For small $\epsilon\,(= 0.25)$, figure 1 shows two main first-order resonant peaks near the plane wave frequencies $f_1 = 2.25$ Hz and $f_2 = 3.55$ Hz. The experimental data follow quite closely Mei's (1985) first-order theoretical predictions, particularly in respect to the position and width of the two peaks. For large ϵ (figure 2, $\epsilon = 0.40$), the experimental peaks are shifted towards lower frequencies compared with the prediction of the first-order theory. In addition, two new small peaks occur, corresponding to second-order Bragg reflections near the plane wave frequencies $f_+ = 4.32$ Hz and $f_{2+} = 5.07$ Hz. These peaks are not predicted by the first-order theory.

As a general trend, peak amplitude and width increase with ϵ. Since $M = 4$ for the results in figures 1 and 2, only a few oscillations in R appear between the main resonant peaks. As ϵ increases, the experimental peak locations are shifted toward lower frequencies compared to the peak locations given by the plane wave frequencies of the Bragg resonances. In contrast, the peak locations given by the first-order theory are in good agreement with the peak locations given by the plane wave frequencies of the Bragg resonances.

Results obtained for the same bed type S_1 but with a larger length $L = 192$ cm (i.e.

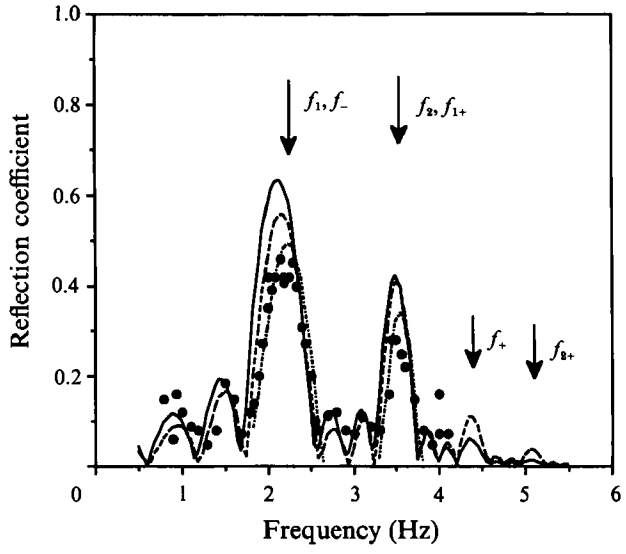

FIGURE 1. Results for the reflection coefficient of bed S_1 with $L = 48$ cm and $\epsilon = \Delta H/H_0 = 0.25$ ($H_0 = 4$ cm). The dots are the experimental data. The solid curve is the present numerical computation taking into account three evanescent modes. The dashed curve is the present numerical computation taking into account no evanescent modes. The first-order analytical results of Mei are shown by a dashed dotted curve.

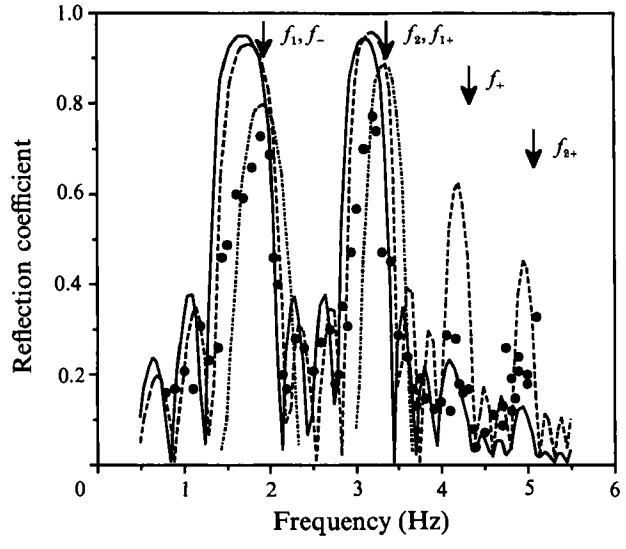

FIGURE 2. As for figure 1, but for $\epsilon = \Delta H/H_0 = 0.40$ ($H_0 = 2.5$ cm).

$M = 16$ for the larger wavelength Λ_1) are shown in figures 3 and 4, for the same values of ϵ. The remarks made above are again applicable as far as the shift toward lower frequencies, and the occurrence of the second-order resonant peaks are concerned. However, many more oscillations are now present between the main resonant peaks, as expected. Moreover, peak amplitude increases and peak width decreases when increasing M for fixed ϵ. This is particularly well demonstrated by comparing figures 1 and 3.

In all the cases of both $M = 4$ and $M = 16$ with bed S_1, good agreement is obtained between the measurements and the numerical calculations obtained with three

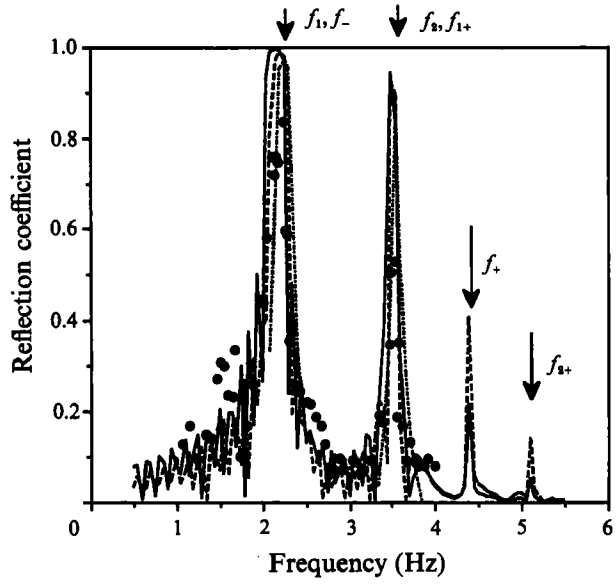

FIGURE 3. Results for the reflection coefficient of bed S_1 with $L = 192$ cm and $\epsilon = \Delta H/H_0 = 0.25$ ($H_0 = 4$ cm). Symbols as for figure 1.

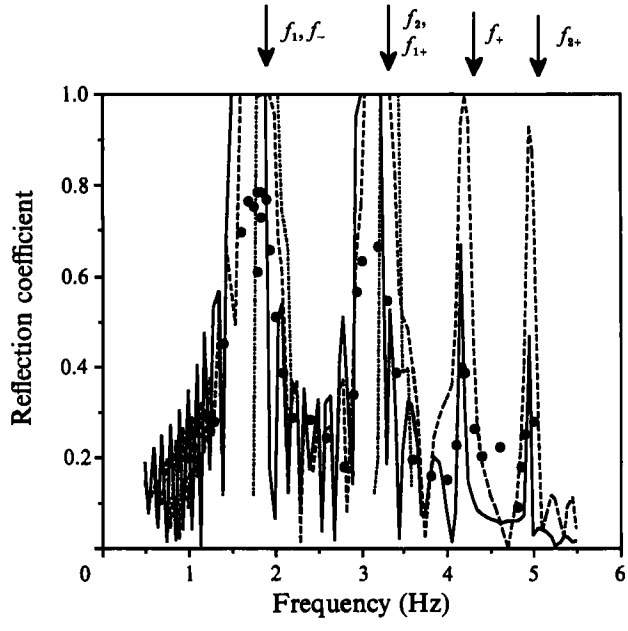

FIGURE 4. As figure 3, but for $\epsilon = \Delta H/H_0 = 0.40$ ($H_0 = 2.5$ cm).

evanescent modes. Both peak positions and widths are well predicted. The increase of the amplitude of a given peak with ϵ and M is also well described. For large M and ϵ (figure 4), perfect reflection is predicted by the model. On the other hand, the results computed with no evanescent modes (broken lines) are not in such good agreement. Prediction of the model without evanescent modes overestimates the higher-order harmonic peak amplitude. This is well evidenced on figures 2 and 4. When ϵ is increased, peaks computed with three evanescent modes are shifted towards lower frequencies compared with peaks predicted without evanescent modes.

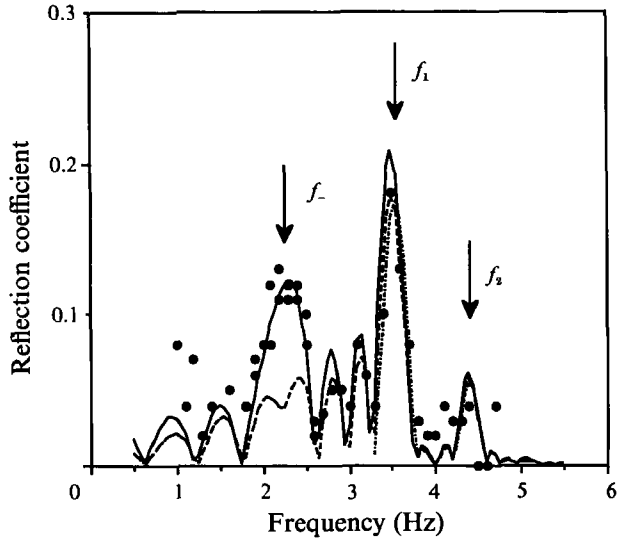

FIGURE 5. Results for the reflection coefficient of bed S_2 with $L = 48$ cm and $\epsilon = \Delta H/H_0 = 0.13$ ($H_0 = 4$ cm). Symbols as for figure 1.

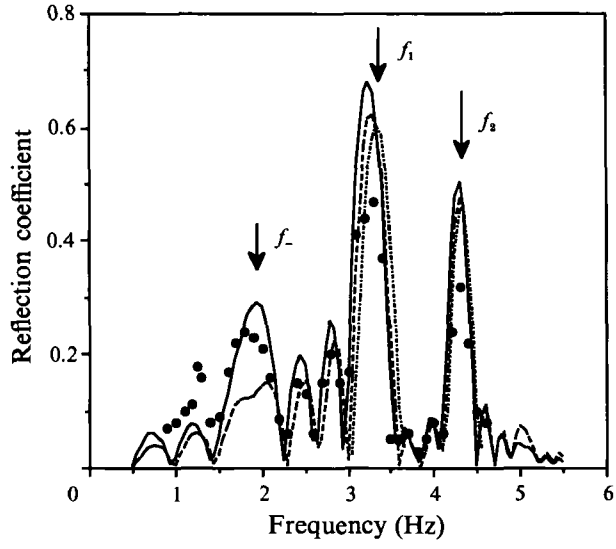

FIGURE 6. As figure 5, but for $\epsilon = \Delta H/H_0 = 0.20$ ($H_0 = 2.5$ cm).

4.2. *Reflection coefficients for the beds S_2 and S_3 with $K_1 = \frac{2}{3}K_2$*

Further experiments were performed with the two-frequency beds S_2 and S_3, for which the wavelengths Λ_1 and Λ_2 were chosen not to be a simple multiple of one another as for bed S_1. The wavelengths were such that the subharmonic resonance associated with $k = \frac{1}{2}(K_2 - K_1)$ (corresponding to frequency f_-) could be observed in the low-frequency range. Higher-order harmonic resonances will not be addressed here since they occur at higher frequencies for the specific bottoms used in this experiment. Indeed, at high frequencies, the bottom has very little influence on wave propagation. Results with a bed length $L = 48$ cm (i.e. $M = 8$ for the larger wavelength Λ_1) are shown in figures 5 and 6 for bed S_2 and in figures 7 and 8 for bed S_3, for the same increasing values of mean water depth as in the experiments of §4.1.

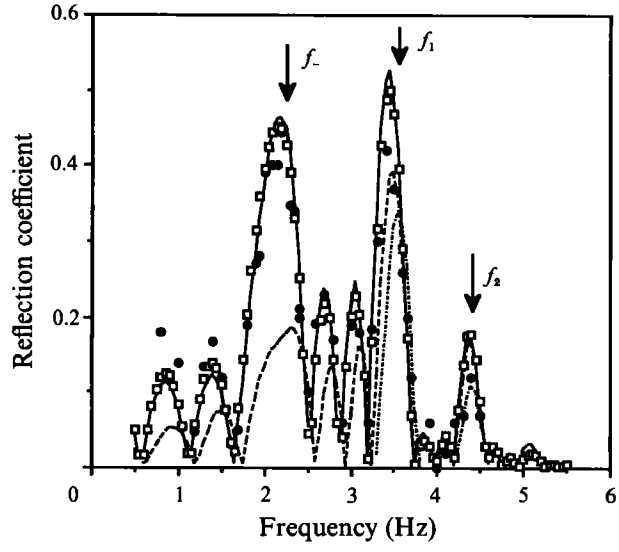

FIGURE 7. Results for the reflection coefficient of the bed S_3 with $L = 48$ cm and $\epsilon = \Delta H/H_0 = 0.25$ ($H_0 = 4$ cm). The solid curve is the present numerical computations taking into account three evanescent modes with a bed subdivision at the maximum slope as in the other figures. The open squares are results of the same numerical computation taking into account three evanescent modes with a bed subdivision at the trough. Other symbols as for figure 1.

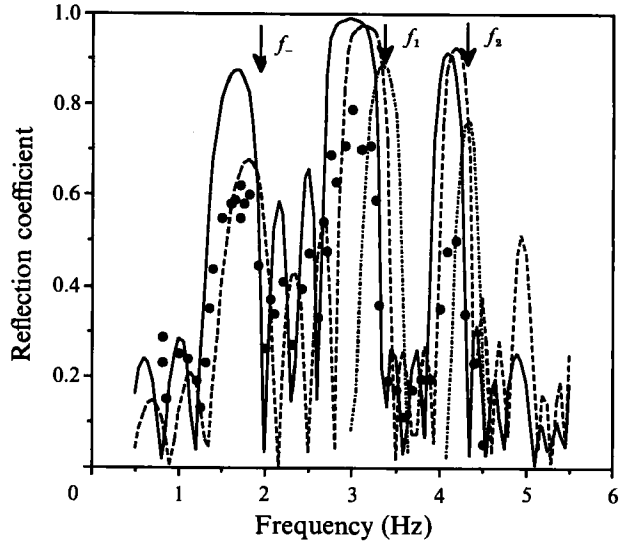

FIGURE 8. As for figure 7, but for $\epsilon = \Delta H/H_0 = 0.40$ ($H_0 = 2.5$ cm).

Again, data corresponding to an intermediate value of relative bed amplitude are not presented here since they showed a continuous behavioral change between the two extreme values.

Consider, firstly, the bed S_2. For small ϵ ($= 0.13$), figure 5 shows the two first-order resonant peaks and the subharmonic peaks which are located in the vicinity of the corresponding plane wave resonance frequencies $f_1 = 3.55$ Hz, $f_2 = 4.41$ Hz and $f_- = 2.25$ Hz. Clearly, the subharmonic peak is very large, which cannot be predicted by Mei's (1985) first-order analytic theory. In contrast, the first-order peaks near f_1

and f_2 follow closely the first-order theory predictions. For large ϵ (figure 6, $\epsilon = 0.20$), the experimental peak amplitudes located near the frequencies $f_1 = 3.35$ Hz, $f_2 = 4.33$ Hz and $f_- = 1.93$ Hz are increased and the experimental peaks are slightly shifted towards low frequency compared with the prediction of the first-order theory.

Consider, secondly, bed S_3. For relatively small $\epsilon (= 0.25)$, figure 7 shows the two first-order resonant peaks near the corresponding plane wave frequencies $f_1 = 3.55$ Hz and $f_2 = 4.41$ Hz and also the second-order subharmonic peak near the corresponding plane wave frequency $f_- = 2.25$ Hz. This second-order peak is again very large and is not predicted by the first-order theory. Even for this small ϵ, the first-order experimental peaks are shifted towards lower frequencies compared to the predictions of the first-order theory and to the peak locations given by the plane wave frequencies of the Bragg resonances. For larger ϵ (figure 8, $\epsilon = 0.40$), the effect of the shift increases. The experimental peak locations are strongly shifted towards low frequencies compared to the peak location given by the plane wave frequencies of the Bragg resonances, $f_1 = 3.35$ Hz and $f_2 = 4.33$ Hz and $f_- = 1.93$ Hz. This shift also increases as f decreases. Again, as a general trend, peak amplitude and width increase with ϵ.

In all of the above cases, good agreement is obtained between the experimental and the numerical calculations taking into account three evanescent modes. Both peak positions and widths are well predicted. On the other hand, the results computed with no evanescent modes (broken lines), are again in poor agreement with the experimental data. This is particularly evident in the vicinity of the subharmonic peak. The predictions of the model without evanescent modes underestimate the subharmonic peak amplitude. As a general rule, the disagreement increases with decreasing frequency, particularly in respect to the subharmonic peak amplitude and to the peak position. Indeed, the experimental data are shifted towards low frequencies compared with the prediction of the model without evanescent modes. This shift increases both with increasing relative bed modulation ϵ and with decreasing frequency for a given bed. This is clearly shown in figures 7 and 8.

5. Discussion and concluding remarks

Measurements of linear gravity waves propagating over doubly sinusoidal beds provided experimental evidence of higher-order subharmonic and harmonic resonant reflection. Subharmonic resonant reflection was found to be very large, even for small relative bed amplitudes. In contrast, higher-order harmonic resonant reflections were revealed successively as the relative bed amplitude was increased. As a general trend, as bed relative amplitude increased, peak amplitude and width increased and experimental peak location shifted towards lower frequencies compared with peak location given by the plane wave Bragg conditions and first-order theory predictions. This shift slightly increased with decreasing wave frequency. Moreover, peak amplitude increased and peak width decreased for beds of increasing spatial period number.

These new higher-order Bragg effects cannot be predicted by the first-order theories for bed relative amplitude. The experimental data were compared with a numerical model based on the linear potential theory derived from Takano (1960) and Kirby & Dalrymple (1983). Results of a simulation, which takes into account evanescent modes, are in fairly good agreement with the experimental data, particularly in respect to peak positions and widths. In the middle-frequency range, where experimental uncertainties are small, the amplitude of the computed peaks

tends to be slightly larger than experimental data. This slight lack of quantitative agreement is thought to be due to the viscous dissipation which is not taken into account in the model. For low and high frequencies, the numerical computation provides predictions within the range of experimental uncertainties which are rather large in this case. Peak amplitude behaviour for increasing bed amplitude is in agreement with that numerically predicted by Mattioli (1991) by means of the same model (see in particular, figure 7 of Mattioli 1991). Furthermore, we found that peak amplitude increases and peak width decreases for beds of increasing spatial period number, M. Computed peak amplitudes are shown to converge to the limit value of 1 when M increases (Belzons *et al.* 1991). This perfect reflection for a large bed was also predicted by Mei's (1985) first-order theory.

In contrast, results of the simulation without evanescent modes are in poor agreement with the experimental data. This is particularly evident in the vicinity of the second-order resonant reflections. Predictions with no evanescent mode underestimate subharmonic peak amplitude (figures 5–8) and overestimate higher-order harmonic peak amplitude (figures 1–4). In addition, the experimental peaks are shifted towards lower frequencies compared with the prediction of the model without evanescent modes. This effect is particularly strong for beds S_2 and S_3 where subharmonic reflection is observed in the low-frequency range. These results confirm the numerical predictions of Mattioli (1991) who investigated the role of evanescent mode inclusion in the resonant reflection phenomenon for doubly sinusoidal beds of similar component wavenumber ratios (see in particular, figures 3 and 4 of Mattioli 1991). We also found that the peak shift increases as the wave frequency decreases.

The present study confirms and extends the numerical results of Mattioli (1991). Comparison between experimental and numerical results shows that the evanescent modes play an important role since only the numerical computation including evanescent modes can predict correctly the higher-order resonant reflection observed experimentally. Indeed, the inclusion of the evanescent modes causes the wave to depart from the plane wave solution and, similarly, the peak locations to depart from their plane wave behaviour. This can be understood by the fact that the propagating waves involved in the Bragg phase matching condition have their amplitudes and phases continuously renormalized by the evanescent modes. Therefore, the evanescent modes fully participate in the phase matching and thus in the interference process. Further investigations related to this last point are presented in Belzons *et al.* (1991).

This work also provides further insight into the importance of subharmonic Bragg reflection. Indeed, although it was expected to be a second-order effect in bed relative amplitude, subharmonic Bragg reflection was found to be very large compared with first-order reflections, even for small relative bed amplitudes. In contrast, as expected, higher-order harmonic resonances were revealed successively as the relative bed amplitude was increased. This original finding can be explained by the following considerations. Firstly, the interaction effect between the wave and the bottom increases as kH_0 diminishes. Therefore, resonant interactions increase with decreasing wave frequency. Secondly, the bottom regions of large steepness are coupled to first order for the subharmonic resonance frequency. Thirdly, the parameter describing the weight of the evanescent modes is of the order of $(\mathrm{d}H/\mathrm{d}x)^2/(kH_0)^2$ (Smith & Sprinks 1975; see also Mei 1983, chap. 3). This parameter shows the role of the steepness of the bottom as well as the increasing influence of the evanescent modes with decreasing frequency. Therefore, the participation of the evanescent modes in the interference process is enhanced for a given bed when

frequency increases and for a fixed frequency when relative bottom amplitude increases.

Much of this work is based upon the thesis research of V. Rey. Some of the preliminary experiments benefited from the stay in our laboratory of L. N'Ganga. We would like to thank A. G. Davies and T. O'Hare for helpful comments and C. C. Mei for fruitful discussions as well as communications of results prior to publication. This work was partially supported by a Convention DRET-Université de Provenance under contract no. 87/112.

REFERENCES

ABRAMOWITZ, M. & STEGUN, A. 1965 *Handbook of Mathematical Functions*. Dover.

BAILLARD, J. A., DEVRIES, J. & KIRBY, J. T. 1992 Considerations in using Bragg reflection for storm erosion protection. *J. Waterway, Port, Coastal Ocean Engng* **118**, 62–74.

BAILARD, J. A., DEVRIES, J., KIRBY, J. T. & GUZA, R. T. 1990 Bragg reflection breakwater: a new shore protection method? *Proc. 22nd Coastal Engng Conf., New York*, pp. 1702–1715. ASCE.

BELZONS, M., GUAZZELLI, E. & PARODI, O. 1988 Gravity wave on a rough bottom: experimental evidence of one-dimensional localization. *J. Fluid Mech.* **186**, 539–558.

BELZONS, M., REY, V. & GUAZZELLI, E. 1991 Subharmonic Bragg resonance for surface water waves. *Europhys. Lett.* **16**, 189–194.

BENJAMIN, T. B., BOCZAR-KARAKIEWICZ, B. & PRITCHARD, W. G. 1987 Reflection of water waves in a channel with corrugated bed. *J. Fluid Mech.* **185**, 249–274.

CARTER, T. G., LIU, P. L.-F. & MEI, C. C. 1973 Mass transport by waves and offshore sand bedforms. *J. Waterways, Harbours, Coastal Engng Div. ASCE* **99**, 165–184.

DALRYMPLE, R. A. & KIRBY, J. T. 1986 Water waves over ripples. *J. Waterway Port Coastal Ocean Engng Div. ASCE* **112**, 309–319.

DAVIES, A. G. 1982*a* The reflection of the wave energy by undulations of the seabed. *Dyn. Atmos. Oceans* **6**, 207–232.

DAVIES, A. G. 1982*b* On the interaction between surface waves and undulations of the seabed. *J. Mar. Res.* **40**, 331–368.

DAVIES, A. G., GUAZZELLI, E. & BELZONS, M. 1989 The propagation of long waves over an undulating bed. *Phys. Fluids* A 1, 1331–1340.

DAVIES, A. G. & HEATHERSHAW, A. D. 1984 Surface wave propagation over sinusoidally varying topography. *J. Fluid Mech.* **144**, 419–443.

DEVILLARD, P., DUNLOP, F. & SOUILLARD, B. 1988 Localization of gravity waves on a channel with random bottom. *J. Fluid Mech.* **186**, 521–538.

GUAZZELLI, E. 1986 Deux études expérimentales du désordre en hydrodynamique physique: désordre spatial de structures convectives; effet du désordre sur la propagation d'ondes de gravité. Thèse d'Etat, Université de Provence, Marseille.

HARA, T. & MEI, C. C. 1987 Bragg scattering of surface waves by periodic bars: theory and experiment. *J. Fluid Mech.* **178**, 221–241.

HEATHERSHAW, A. D. 1982 Seabed–wave resonance and sand bar growth. *Nature* **296**, 343–345.

HEATHERSHAW, A. D. & DAVIES, A. G. 1985 Resonant wave reflection by transverse bedforms and its relation to beaches and offshore bars. *Mar. Geol.* **62**, 321–338.

JAGGARD, D. L. & JORDAN, A. K. 1984 Inversion theory for almost periodic media. *Radio Sci.* **19**, 1333–1341.

KIRBY, J. T. 1986 A general wave equation for waves over rippled beds. *J. Fluid Mech.* **162**, 171–186.

KIRBY, J. T. 1989 Propagation of surface waves over undulating bed. *Phys. Fluids* A 1, 1898–1899.

KIRBY, J. T. & ANTON, J. P. 1990 Bragg reflection of waves by artificial bars. *Proc. 22nd Coastal Engng Conf., New York*, pp. 757–768. ASCE

KIRBY, J. T. & DALRYMPLE, R. A. 1983 Propagation of obliquely incident water waves over a trench. *J. Fluid Mech.* **133**, 47–63.

KITTEL, C. 1976 *Introduction to Solid State Physics*, 5th Edn. Wiley.

MATTIOLI, F. 1990 Resonant reflection of a series of submerged breakwaters. *Il Nuovo Cimento* **13**, 823–833.

MATTIOLI, F. 1991 Resonant reflection of surface waves by non-sinusoidal bottom undulations. *Appl. Ocean Res.* **13**, 49–53.

MEI, C. C. 1983 *The Applied Dynamics of Ocean Surface Waves*. John Wiley.

MEI, C. C. 1985 Resonant reflection of surface waves by periodic sandbars. *J. Fluid Mech.* **152**, 315–335.

MEI, C. C. & BLACK, J. L. 1969 Scattering of surface waves by rectangular obstacle in waters of finite depth. *J. Fluid Mech.* **38**, 499–511.

MILES, J. W. 1967 Surface scattering matrix for a shelf. *J. Fluid Mech.* **28**, 755–767.

MITRA, A. & GREENBERG, M. D. 1984 Slow interactions of gravity waves and corrugated seabed. *Trans. ASME* E: *J. Appl. Mech.* **51**, 251–255.

O'HARE, T. J. & DAVIES, A. G. 1990 A laboratory study of sand bar evolution. *J. Coastal Res.* **6**, 531–544.

O'HARE, T. J. & DAVIES, A. G. 1991 A new model for wave propagation over rapidly-varying bottom. *Coastal Engng* (submitted).

REY, V. 1991 Propagation d'ondes de gravité au dessus de fonds solides ou constitués de sédiments: application à l'étude d'interactions dynamiques ondes-sédiments. Thèse de l'Université de Provence, Marseille.

REY, V. 1992 Propagation and local behaviour of normal incident gravity waves over varying topography. *Eur. J. Mech. B: Fluids* **11**, 213–232.

REY, V., BELZONS, M. & GUAZZELLI, E. 1992 Propagation of surface gravity waves over a rectangular submerged bar. *J. Fluid Mech.* **235**, 453–479.

RHINES, P. B. 1970 Wave propagation in a periodic medium with application to the ocean. *Rev. Geophys. Space Phys.* **8**, 303–319.

SHORT, A. D. 1975 Multiple offshore bars and standing waves. *J. Geophys. Res.* **80**, 3838–3840.

SMITH, R. & SPRINKS, T. 1975 Scattering of surface waves by a conical island. *J. Fluid Mech.* **72**, 373–384.

TAKANO, K. 1960 Effets d'un obstacle parallélépipédique sur la propagation de la houle. *Houille Blanche* **15**, 247–267.

WHITHAM, G. B. 1974 *Linear and Non Linear Waves*. Wiley.